Supplementary material

"Formation of pedestalled, relict lakes on the McMurdo Ice Shelf, Antarctica"

Grant J. Macdonald, Alison F. Banwell, Ian C. Willis, David P. Mayer, Becky Goodsell and Douglas R. MacAyeal

Methods

Classification of 'surface type zones' on McMIS

Based on field observations and analysis of Landsat 7 and 8 imagery, we identified four main surface types on the McMIS: snow/dry firn, thick debris (i.e. the Black Island Medial Moraine), blue ice, and dirty (debris-covered) ice. We used a true-colour pan-sharpened Landsat 8 image from 12 December 2016, which was cloud-free across our area of interest, to perform a supervised classification of surface types. First, we identified pixels of each of the four surface types and assigned them as 'training data'. To maximise the available training data, we sourced training data from areas outside of the area shown in Fig. 1a, in addition to inside it. For example, training data for 'thick debris' included areas on land. Training pixels constituted 2% of total McMIS pixels in the image. Using ArcMap, we then used the training data with a 'minimum distance' supervised classification algorithm to classify every pixel in a multispectral version of the image (bands 1-7) into one of the four surface types. The output of this produced a 'surface-cover classification map' of the McMIS (Fig. S1). The minimum distance algorithm assesses which class of surface type (as defined by the training data) each image pixel is spectrally closest to, based on the spectral signature of all seven bands. The number of training pixels was limited for the blue ice and dirty ice classes because the heterogeneous surface made it difficult to identify large areas consisting solely of that surface type. This is why we used the 'minimum distance' algorithm, as opposed to the 'maximum likelihood' algorithm, because it can perform better when the number of training sites per a class is limited (Richards and Jia, 1999).

Using the surface-cover classification map (Fig. S1) produced by the supervised classification, alongside visual interpretation of the images and reference to the literature, we divided the ice shelf into the Dry Firn Zone, Blue Ice Zone, Debris-Covered Ablation Zone and Channelized Ablation Zone shown in Fig 1a.

Field observations and time-lapse camera

We spent several weeks on the ground in the study area during three deployments: December 2015-January 2016; October-November 2016; and, January-February 2017. We actively explored and photographed the surface, and also made passive observations while undertaking other field activities. Additionally, we observed and photographed the surface of the ice shelf from a helicopter on numerous occasions in both summers.

The time-lapse camera that took the photos in Fig. S2 was a Harbotronics 'Cyclapse' system containing a Canon EOS Rebel T6i camera, which operated from 25 November 2016 until 27 January 2017, taking photos every 30 minutes. The location of the camera is shown in Fig. 1b and it was situated to collect data on Rift Tip Lake, a lake not reported here but reported in Banwell and others (*in press*).

Satellite imagery analysis

All November-February Landsat 7 Enhanced Thematic Mapper Plus (ETM+) and Landsat 8 Operational Land Imager (OLI) images of the study region that were sufficiently cloud-free over the study region shown in Fig. 1b were downloaded, covering the period 13 December 1999 to 19 January 2018. Images with heavy cloud cover could be used for analysis provided that at least one of our features of interest was visible. Landsat was chosen for its high spatial resolution (30 m) compared with the lower spatial resolution of MODIS (250 m).

This period spans the first ETM+ images of the area until the most recent usable OLI image. Between 13 December 1999 and 31 January 2013 the images are captured by ETM+, and between 7 November 2013 and 18 January 2018 they are from OLI. OLI imagery has the advantage of a higher temporal acquisition rate than ETM+ and is free from the issue of missing scanlines that affects ETM+ imagery after May 2003 (as seen in Figs 2d-g). However, given the manual nature of the analysis used in this study, scanlines did not preclude imagery from being useful even when they obscured part of the study site. Additionally, for January-February 2002, which was a particularly important period for analysis, there were no Landsat images, so true-colour corrected surface reflectance MODIS images were analyzed in NASA's Worldview application (e.g. Fig. 2b). These images proved sufficient to at least identify the presence of the surface lake at Peanut Lobe 1 (Fig. 2b). MODIS images were also consulted for the 2005/2006 austral summer (when there were no Landsat images), but these images were difficult to interpret and not useful for analysis.

All true-colour pan-sharpened Landsat images were cropped to the region of interest (Fig. 1b) and assembled into the time-series used to create Video S1. True-colour MODIS images for 2001/02 were similarly cropped and analysed separately. Analysis of the evolution of the pedestal sites and their interaction with the surrounding surface was carried out by manual visual interpretation of the images, with a particular focus on the sites of Ring and Peanut's two lobes. The unique nature of the pedestalled features, and their development from open water surface lakes, did not allow for an automated approach. Given our knowledge of the surface from the ground, manual visual interpretation of the satellite imagery is considered optimal for the purposes of the study.

Topographical survey

The surface profile of Ring Pedestal and its immediate surroundings was measured across two approximately perpendicular transects (locations indicated in Fig. 1b) using a roving Trimble R7 differential GPS provided by UNAVCO. There is 5-10 cm vertical uncertainty in the measurements. One member of the team marked out the route in an approximate straight line. The second member of the team walked, carrying the GPS system and counted their paces. On the surface of the pedestal they logged a measurement approximately every 40 paces (~25-30 m). To better capture the high level of roughness in the area surrounding the pedestal, measurements were logged there approximately every 25 paces (~15-20m). The frequency of measurements logged was limited by time constraints.

We acknowledge that other methods (e.g. terrestrial LIDAR) could characterize the surface topography of the pedestals at a higher spatial resolution and in three dimensions across the site. However, these data were not available to us. We regard these topographical transects sufficient for illustrating the contrast in topography of the pedestal and the surrounding area for the purpose of this study.

Ablation measurements

Mean ablation rates for debris-covered ice and clean ice were calculated from ablation measurements recorded at twelve sites across the study region. The heights of aluminium poles exposed above the snow/firn/ice surface was recorded when they were deployed (5 - 11 November 2016) and again when they were retrieved (21 January – 1 February 2017). Nine poles were located in clean areas, where the ice surface was free of debris, and three where it was debris-covered. All poles were located within the study site (Fig. 1b). Three were located in the vicinity of the time-lapse camera, three on and around Ring Pedestal, three on and around Peanut Lobe 2, and three in a location ~1 km east of Peanut Lobe 2.

Air temperature data

Daily surface air temperature data were acquired from the Antarctic Meteorological Research Center & Antarctic Weather Stations Project's website (http://amrc.ssec.wisc.edu/aws/api/form.html). All data from the Pegasus North AWS station that were available for our period of interest (November 1999 to January 2018) were downloaded. Data existed for all months between November 2001 until December 2013, except for November - December 2008. There were also data for December 2016 – October 2017, except for January and March 2017. The mean temperature was calculated for each month and presented in Fig. S4.

Supplementary figures

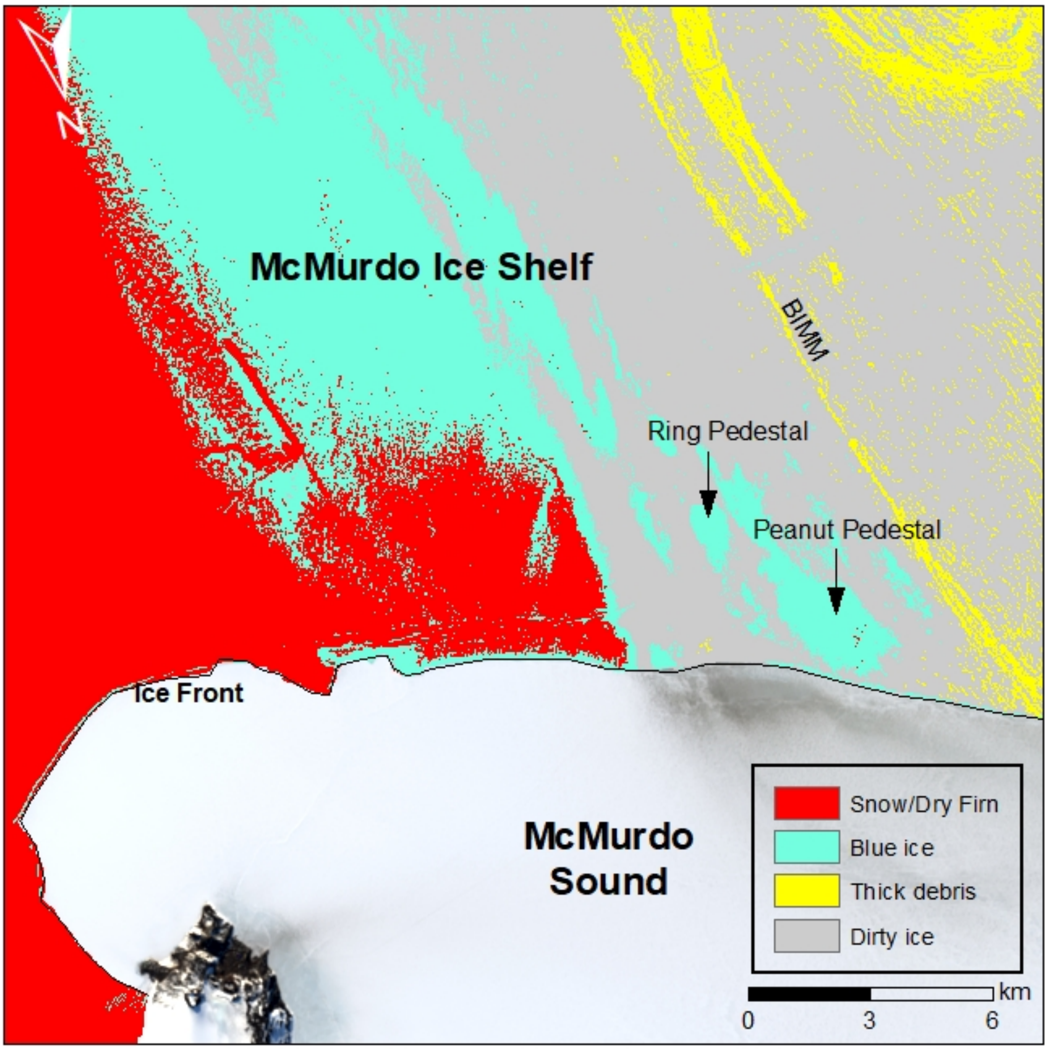

Fig. S1: **Surface-cover map of the McMIS based on a supervised classification analysis.** The four surface types ('Snow/Dry Firn', 'Blue ice', 'Thick debris' and 'Dirty ice') are shown in the key, and were used to define the surface zones labelled in Fig. 1a. The classified image, which is also the background image, is a multispectral OLI image captured on 12 December 2016. The extent of the figure is the same as in Fig 1a. Note that the pedestals are classified as having a ‘blue ice’ surface, similar to that which dominates the Blue Ice Zone.

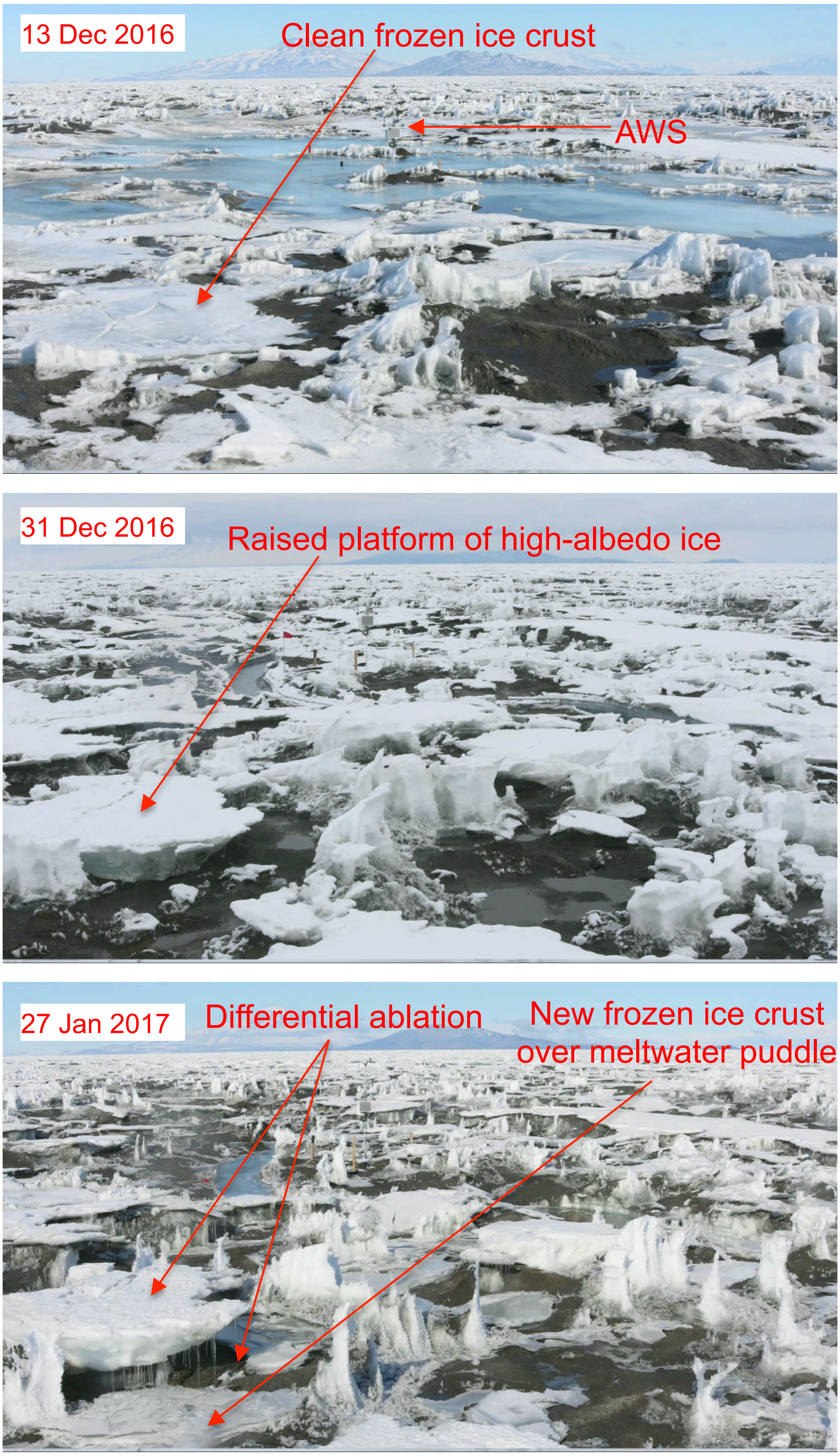

Fig. S2: Time-lapse camera photographs showing the effects of differential ablation at a small scale. The location of the time-lapse camera is shown in Fig. 1a. An AWS is visible in the upper, central area of each photograph.

Figure S3: A pingo on Ring Pedestal in November 2016.

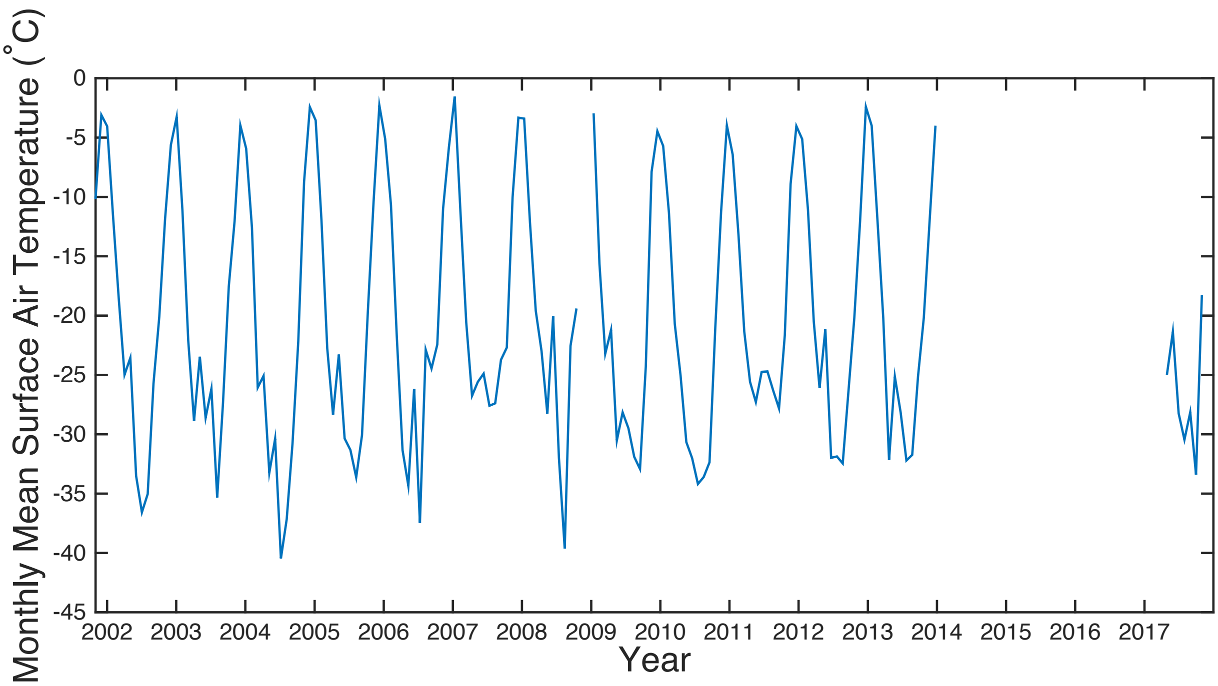

Fig. S4: Mean monthly air temperature at Pegasus North station in the east of the McMIS from November 2001 to November 2017, where data are available.

Table S1: Table of satellite image IDs and dates used to compile the time-series of the formation of pedestals. For each image, we use our best judgement to determine whether Ring, Peanut Lobe 1, and Peanut Lobe 2 are 'open water' surface lakes, 'frozen over' lakes or 'pedestalled'. '/' indicates that the feature does not yet exist in any form (i.e. there is bare ice/firn). '*' indicates that there is a ring of meltwater at the edge of the feature, as in Fig. 2f. As we discuss in the text, it is not clear at this point whether the lake is 'frozen over' or 'pedestalled'.

Supplementary Video 1: The complete time-series of 147 Landsat images from 13 December 1999 to 18 January 2018

Supplementary reference:

Richards, J.A. & Jia, X. (1999) Remote sensing digital image analysis. An Introduction. 3rd Edition. *Springer*, Berlin, Heidelberg, New York, 363pp